

# Low-Temperature Rate Coefficients of C<sub>2</sub>H with CH<sub>4</sub> and CD<sub>4</sub> from 154 to 359 K

Brian J. Opansky and Stephen R. Leone\*,†

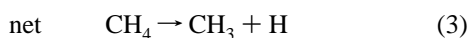
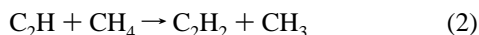
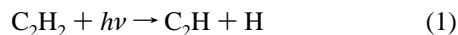
*JILA, National Institute of Standards and Technology and University of Colorado, Department of Chemistry and Biochemistry, University of Colorado, Boulder, Colorado 80309-0440*

*Received: November 6, 1995; In Final Form: January 2, 1996*<sup>®</sup>

Rate coefficients for the reaction C<sub>2</sub>H + CH<sub>4</sub> → C<sub>2</sub>H<sub>2</sub> + CH<sub>3</sub> and C<sub>2</sub>H + CD<sub>4</sub> → C<sub>2</sub>HD + CD<sub>3</sub> are measured over the temperature range 154–359 K using transient infrared laser absorption spectroscopy. Ethynyl radicals are produced by pulsed laser photolysis of C<sub>2</sub>H<sub>2</sub> in a variable temperature flow cell, and a tunable color center laser probes the transient removal of C<sub>2</sub>H (X<sup>2</sup>Σ<sup>+</sup> (0,0,0)) in absorption. The rate coefficients for the reactions of C<sub>2</sub>H with CH<sub>4</sub> and CD<sub>4</sub> both show a positive temperature dependence over the range 154–359 K, which can be expressed as  $k_{\text{CH}_4} = (1.2 \pm 0.1) \times 10^{-11} \exp[(-491 \pm 12)/T]$  and  $k_{\text{CD}_4} = (8.7 \pm 1.8) \times 10^{-12} \exp[(-650 \pm 61)/T] \text{ cm}^3 \text{ molecule}^{-1} \text{ s}^{-1}$ , respectively. The reaction of C<sub>2</sub>H + CH<sub>4</sub> exhibits a significant kinetic isotope effect at 300 K of  $k_{\text{CH}_4}/k_{\text{CD}_4} = 2.5 \pm 0.2$ . Temperature dependent rate constants for C<sub>2</sub>H + C<sub>2</sub>H<sub>2</sub> were also remeasured over an increased temperature range from 143 to 359 K and found to show a slight negative temperature dependence, which can be expressed as  $k_{\text{C}_2\text{H}_2} = 8.6 \times 10^{-16} T^{1.8} \exp[(474 \pm 90)/T] \text{ cm}^3 \text{ molecule}^{-1} \text{ s}^{-1}$ .

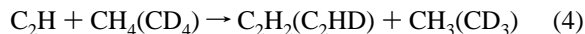
## Introduction

This work is part of an ongoing project to measure, for the first time, low-temperature rate constants of the C<sub>2</sub>H radical with various hydrocarbons present in Titan's atmosphere. In planetary atmospheres, such as Titan's, the ethynyl radical can catalyze the dissociation of CH<sub>4</sub> to form methyl radicals, CH<sub>3</sub>.<sup>1,2</sup>



The recombination of two methyl radicals produces ethane, C<sub>2</sub>H<sub>6</sub>, which can be transported downward to the moon's surface. Hence, the reaction C<sub>2</sub>H + CH<sub>4</sub> is of central importance in photochemical models of Titan to understand why ethane is so abundant in Titan's atmosphere.<sup>1,2</sup>

This is the first low-temperature study of the reactions



over the temperature range 154–359 K. A complete study of the reaction C<sub>2</sub>H + C<sub>2</sub>H<sub>2</sub> from 170 to 350 K, another critical reaction in Titan's atmosphere, was already reported by this laboratory;<sup>3</sup> here, these measurements have also been extended to 143–359 K. Low-temperature rate constants of reaction 4 will help decide which reaction schemes for ethane production are consistent with data from Voyager IRIS (infrared interferometer spectrometer) results.<sup>4,5</sup> In addition, NASA plans to launch a mission called Cassini, which is intended to study Saturn and its moon Titan some time in 1996. The rate coefficients measured in this experiment will be used to model Titan's atmosphere to compare calculated gas densities with measured concentrations from the Cassini mission. In addition,

<sup>†</sup> Staff Member, Quantum Physics Division, National Institute of Standards and Technology.

<sup>®</sup> Abstract published in *Advance ACS Abstracts*, March 1, 1996.

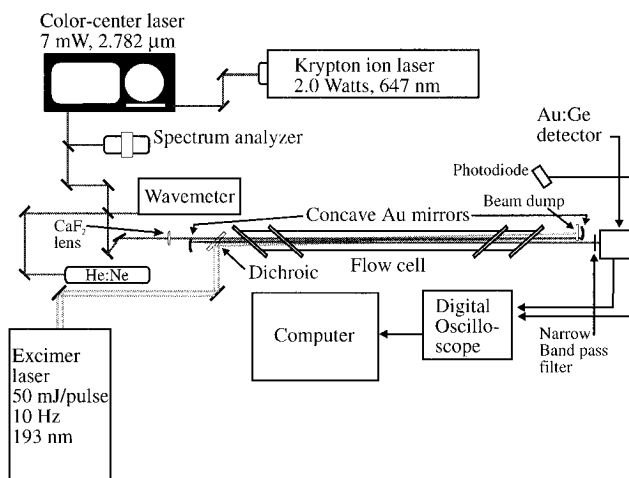


Figure 1. Schematic of the experimental setup.

these results provide an experimental basis for theoretical studies on primary isotope effects.

## Experimental Technique

Briefly, the kinetics of C<sub>2</sub>H + CH<sub>4</sub> and CD<sub>4</sub> are studied using transient infrared laser absorption spectroscopy. A schematic of the experimental setup is shown in Figure 1. The low-temperature kinetics measurements are described in detail in an earlier paper.<sup>6</sup> The only significant change was to add Brewster windows to the flow cell to incorporate a multipass arrangement for the probe laser beam to increase the absorption path length.

Ethynyl radicals are produced in the meter long variable temperature flow cell by a pulsed excimer laser at 193 nm. The excimer laser was operated at 55 mJ/pulse at a repetition rate of 10 Hz. Acetylene has an absorption cross section of  $1.35 \times 10^{-19} \text{ cm}^2$  at 193 nm<sup>7</sup> and a quantum yield of approximately 0.26 for C<sub>2</sub>H production.<sup>8</sup> After accounting for UV laser loss on the windows and absorption in air, the C<sub>2</sub>H concentration was calculated to be no greater than  $4.6 \times 10^{10} \text{ cm}^{-3}$  for the highest acetylene pressures (the acetylene number density was

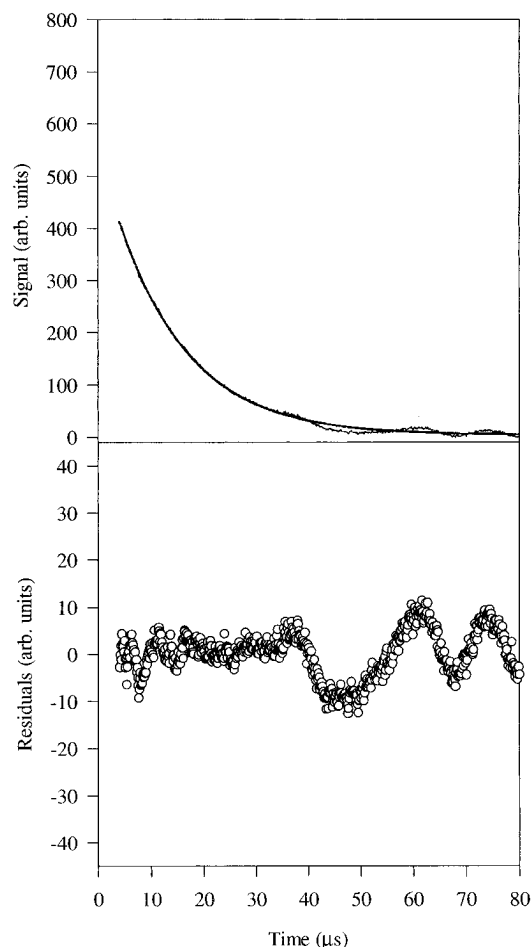


**Figure 2.** (a) Decay of C<sub>2</sub>H with C<sub>2</sub>H<sub>2</sub>. The solid line is the fitted single-exponential decay. (b) Residuals to the fit. The oscillations at lower frequencies are due to the noise from the color center laser.

in the range  $(1.6\text{--}6.4) \times 10^{14} \text{ cm}^{-3}$  in the CH<sub>4</sub> (CD<sub>4</sub>) experiments). For these experiments a 1000–1500-fold excess of CH<sub>4</sub> (CD<sub>4</sub>) with respect to C<sub>2</sub>H<sub>2</sub> is always present. Contributions from secondary or radical–radical reactions can be neglected since the time between collisions for C<sub>2</sub>H and CH<sub>4</sub> (CD<sub>4</sub>) is 1000 times shorter than the time between collisions of two C<sub>2</sub>H radicals. The transverse flow arrangement in the cell allows high laser repetition rates with minimal photolysis of the same gas volume. With typical linear flow rates of  $1.9 \times 10^{20} \text{ molecules s}^{-1}$ , about 90% of which is helium, the photolysis volume is replenished every 10 laser pulses. Kinetic experiments are performed at various methane (methane-*d*) densities  $((0.2\text{--}2.5) \times 10^{17} \text{ cm}^{-3})$ . The total helium density is in the range  $(0.4\text{--}2.4) \times 10^{18} \text{ cm}^{-3}$ , and the methane density is held at  $0.7 \times 10^{17} \text{ cm}^{-3}$  to test for a pressure dependence. In the experiments involving just the reaction C<sub>2</sub>H + C<sub>2</sub>H<sub>2</sub>, the acetylene number density was in the range  $(0.2\text{--}6.0) \times 10^{15} \text{ cm}^{-3}$ , and the helium number density was in the range  $(0.32\text{--}3.2) \times 10^{18} \text{ cm}^{-3}$ . For the highest acetylene pressures, the C<sub>2</sub>H concentration is estimated to be no greater than  $6.7 \times 10^{11} \text{ cm}^{-3}$ . Therefore, a 300–9000-fold excess of C<sub>2</sub>H<sub>2</sub> with respect to C<sub>2</sub>H is always present. Contributions from radical–radical reactions can be neglected since the time between collisions for two C<sub>2</sub>H radicals is 1000 times longer at the highest C<sub>2</sub>H density than the time between collisions for C<sub>2</sub>H and C<sub>2</sub>H<sub>2</sub>.

A high-resolution color center laser tuned to the Q<sub>11</sub>(9) line at  $3593.68 \text{ cm}^{-1}$  of the A <sup>2</sup>Π–X <sup>2</sup>Σ transition probes the transient concentration of ethynyl radical in absorption.<sup>9</sup> A scanning Fabry–Perot spectrum analyzer is used to ensure that the color center is running on one longitudinal mode, and a

home-built scanning Michelson interferometer wavemeter<sup>10</sup> is used to monitor the color center's wavelength.

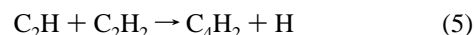
The probe beam, after three to five multipasses, is directed onto a 50-MHz 77 K Ge:Au detector which has a 20-mm<sup>2</sup> sensitive area. The transient signals are amplified and then coadded using a 100-MHz digital oscilloscope. Typical single-shot traces have a signal-to-noise ratio of 20–30. For a typical run, transient signals from 1000 excimer pulses are averaged. The amplitude of the transient C<sub>2</sub>H signal is found to be linear with color center probe power.

In all experiments, acetylene, helium, and methane or methane-*d*<sub>4</sub> were flowed through a mixing cell before entering the reaction cell. Helium is used to thermally equilibrate the mixture with the cell walls. In earlier experiments, sulfur hexafluoride, SF<sub>6</sub>, was used to vibrationally and electronically quench the C<sub>2</sub>H;<sup>3,6</sup> this was omitted from this study because it was found to have no effect on the relatively slow ground-state removal rates, as discussed below. All gases are obtained commercially with the following purities: He, 99.99%; C<sub>2</sub>H<sub>2</sub>, 99.6%; CH<sub>4</sub>, 99.99%; CD<sub>4</sub>, 99.6%. The acetone in the C<sub>2</sub>H<sub>2</sub> is removed by passing the gas through an activated charcoal filter. Partial pressures of each gas are determined by calibrated mass flow meters and the measured total pressure inside the cell. With the use of isopentane as a cooling solvent, temperatures as low as 143 K can be reached. For measurements taken above 300 K, heated water was used as the solvent.

### Analysis of Kinetic Data

In this study we observe reactions from the ground state of C<sub>2</sub>H (X<sup>2</sup>Σ<sup>+</sup> (0,0,0)) directly. For accurate measurements it is necessary that the electronic and vibrationally excited states of C<sub>2</sub>H be fully quenched. Work done by Glass *et al.* under similar conditions reports that relaxation of the C<sub>2</sub>H (X(0,0,1)) state occurs in approximately 1 μs.<sup>9</sup> Therefore, if sufficient time has elapsed, complete vibrational and electronic relaxation should have occurred before any ground-state measurements are made. The data is fit only beginning with times a factor of 3 longer than the rise time to ensure complete relaxation of upper vibrational states of C<sub>2</sub>H. In previous studies SF<sub>6</sub> was used as a vibrational quencher.<sup>3,6</sup> Temperature dependent measurements with and without SF<sub>6</sub> were taken, and the measured rate constants were found to be equal. Therefore, SF<sub>6</sub> was not used for this study.

Prior to measuring rate coefficients for the reaction C<sub>2</sub>H + CH<sub>4</sub> (CD<sub>4</sub>), an accurate temperature dependence investigation of the rate constant for



had to be completed. Earlier measurements could only be made down to 170 K, and here it was desired to extend the results to at least 143 K.<sup>3</sup> The experiments were done under pseudo-first-order conditions where  $[\text{C}_2\text{H}_2] \gg [\text{C}_2\text{H}]$  by a factor of 500–1500. The rate equation for reaction 5 integrates to

$$[\text{C}_2\text{H}]_t = [\text{C}_2\text{H}]_0 \exp(-k_{\text{obs}}t) \quad (6)$$

where

$$k_{\text{obs}} = k_{\text{C}_2\text{H}_2}[\text{C}_2\text{H}_2] \quad (7)$$

The observed rate coefficients,  $k_{\text{obs}}$ , are calculated by fitting the observed decay traces to a single-exponential decay plus a constant, eq 8, to fit the zero level of the base line

$$y = A \exp(-k_{\text{obs}}t) + \text{constant} \quad (8)$$

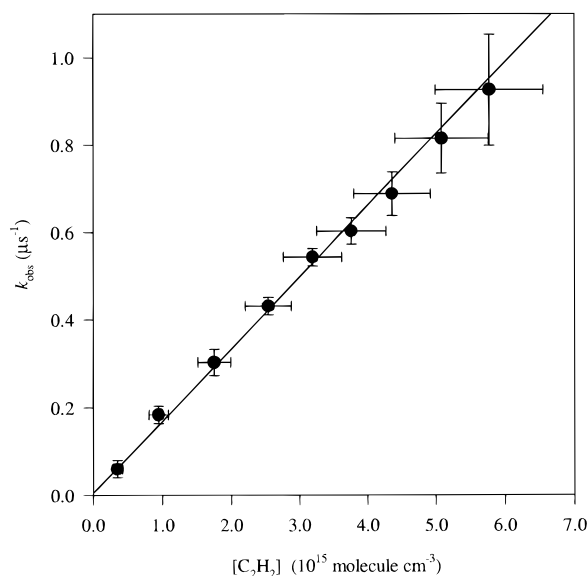


**Figure 3.** Plot of observed  $\text{C}_2\text{H}$  removal coefficient  $k_{\text{obs}}$  versus  $\text{C}_2\text{H}_2$  concentration. These data were taken at 155 K, and  $k_{\text{C}_2\text{H}_2}$  for this plot is  $(1.6 \pm 0.2) \times 10^{-10} \text{ cm}^3 \text{ molecule}^{-1} \text{ s}^{-1}$ .

where  $A$  is the pre-exponential factor,  $t$  is the time, and  $k_{\text{obs}}$  is the observed rate coefficient; see Figure 2. The fits for  $k_{\text{obs}}$  are then plotted against their respective  $[\text{C}_2\text{H}_2]$  concentrations, and the gradient is  $k_{\text{C}_2\text{H}_2}$ ; see Figure 3. The uncertainty in  $k_{\text{C}_2\text{H}_2}$  is calculated on the basis of the uncertainties in fitting  $k_{\text{obs}}$ , measuring  $[\text{C}_2\text{H}_2]$ , and measuring the temperature. This leads to relative errors in  $k_{\text{C}_2\text{H}_2}$  of 10–13%, depending on the temperature.

Table 1 is a summary of the rate constants measured for  $\text{C}_2\text{H} + \text{C}_2\text{H}_2$  down to 143 K. The data from ref 3 and the new data can be fit approximately to the Arrhenius equation. However, the data is best fit by the equation  $k_{\text{C}_2\text{H}_2} = 8.6 \times 10^{-16} T^{1.8} \exp[(474 \pm 90)/T] \text{ cm}^3 \text{ molecule}^{-1} \text{ s}^{-1}$ ; see Figure 4.

All experiments involving methane were performed under pseudo-first-order conditions in which  $[\text{CH}_4]$ ,  $[\text{CD}_4]$ , and  $[\text{C}_2\text{H}_2] \gg [\text{C}_2\text{H}]$ . The rate of change of  $[\text{C}_2\text{H}]$  can be expressed as

$$d[\text{C}_2\text{H}]/dt = -[\text{C}_2\text{H}](k_{\text{CX}_4}[\text{CX}_4] + k_{\text{C}_2\text{H}_2}[\text{C}_2\text{H}_2]) \quad (9)$$

where  $\text{CX}_4 = \text{CH}_4$  or  $\text{CD}_4$ . After integration

$$[\text{C}_2\text{H}]_t = [\text{C}_2\text{H}]_0 \exp(-k_{\text{obs}}t) \quad (6')$$

$$k_{\text{obs}} = k_{\text{CX}_4}[\text{CX}_4] + k_{\text{C}_2\text{H}_2}[\text{C}_2\text{H}_2] \quad (10)$$

$$k_{\text{obs}} - k_{\text{C}_2\text{H}_2}[\text{C}_2\text{H}_2] = k_{\text{CX}_4}[\text{CX}_4] = k'_{\text{CX}_4} \quad (11)$$

The observed decay rates,  $k_{\text{obs}}$ , are obtained by fitting the observed traces to eq 8. They are then corrected for the contribution of the  $\text{C}_2\text{H}_2$  precursor reacting with  $\text{C}_2\text{H}$  using both previous measurements and new measurements down to 143 K, as noted in eq 11. Since  $\text{C}_2\text{H}$  reacts 100 times faster with  $\text{C}_2\text{H}_2$  than it does with  $\text{CX}_4$ , the contribution to  $k_{\text{obs}}$  from  $\text{C}_2\text{H}_2 + \text{C}_2\text{H}$  is kept below 40%. The values of  $k'_{\text{CX}_4}$  are plotted against their respective  $\text{CX}_4$  concentrations, and a linear least squares fit is used to determine  $k_{\text{CX}_4}$ ; see Figure 5. The uncertainty in  $k_{\text{CX}_4}$  is calculated by combining the accumulated uncertainties in the corrected decay fits, which include errors in  $k_{\text{C}_2\text{H}_2}$ , with the uncertainties in temperature and the measurement of  $[\text{CX}_4]$ . The error in  $k_{\text{CX}_4}$  is typically 10–20%.

**TABLE 1: Summary of Rate Constants for  $\text{C}_2\text{H} + \text{C}_2\text{H}_2$  from 143 to 359 K**

temp (K)	$k_{\text{C}_2\text{H}_2}$ ( $\text{cm}^3 \text{ molecule}^{-1} \text{ s}^{-1}$ )	temp (K)	$k_{\text{C}_2\text{H}_2}$ ( $\text{cm}^3 \text{ molecule}^{-1} \text{ s}^{-1}$ )
359 <sup>a</sup>	$(1.3 \pm 0.1) \times 10^{-10}$	211 <sup>b</sup>	$(1.3 \pm 0.2) \times 10^{-10}$
350 <sup>b</sup>	$(1.2 \pm 0.2) \times 10^{-10}$	207 <sup>b</sup>	$(1.3 \pm 0.2) \times 10^{-10}$
296 <sup>a</sup>	$(1.4 \pm 0.1) \times 10^{-10}$	201 <sup>b</sup>	$(1.3 \pm 0.2) \times 10^{-10}$
295 <sup>b</sup>	$(1.3 \pm 0.2) \times 10^{-10}$	199 <sup>b</sup>	$(1.3 \pm 0.2) \times 10^{-10}$
273 <sup>b</sup>	$(1.2 \pm 0.2) \times 10^{-10}$	197 <sup>b</sup>	$(1.4 \pm 0.1) \times 10^{-10}$
263 <sup>b</sup>	$(1.2 \pm 0.2) \times 10^{-10}$	193 <sup>b</sup>	$(1.3 \pm 0.2) \times 10^{-10}$
256 <sup>b</sup>	$(1.3 \pm 0.2) \times 10^{-10}$	193 <sup>b</sup>	$(1.3 \pm 0.2) \times 10^{-10}$
245 <sup>b</sup>	$(1.3 \pm 0.2) \times 10^{-10}$	191 <sup>a</sup>	$(1.5 \pm 0.1) \times 10^{-10}$
242 <sup>b</sup>	$(1.2 \pm 0.2) \times 10^{-10}$	188 <sup>b</sup>	$(1.2 \pm 0.2) \times 10^{-10}$
239 <sup>b</sup>	$(1.3 \pm 0.2) \times 10^{-10}$	185 <sup>b</sup>	$(1.4 \pm 0.2) \times 10^{-10}$
233 <sup>b</sup>	$(1.2 \pm 0.2) \times 10^{-10}$	170 <sup>b</sup>	$(1.4 \pm 0.2) \times 10^{-10}$
232 <sup>b</sup>	$(1.3 \pm 0.2) \times 10^{-10}$	163 <sup>a</sup>	$(1.8 \pm 0.2) \times 10^{-10}$
225 <sup>b</sup>	$(1.2 \pm 0.2) \times 10^{-10}$	155 <sup>a</sup>	$(1.6 \pm 0.2) \times 10^{-10}$
223 <sup>b</sup>	$(1.3 \pm 0.2) \times 10^{-10}$	153 <sup>b</sup>	$(1.8 \pm 0.2) \times 10^{-10}$
223 <sup>b</sup>	$(1.2 \pm 0.2) \times 10^{-10}$	143 <sup>a</sup>	$(1.9 \pm 0.2) \times 10^{-10}$
213 <sup>b</sup>	$(1.4 \pm 0.2) \times 10^{-10}$		

<sup>a</sup> Measurements in this work. <sup>b</sup> Measurements made in a previous study.<sup>3</sup>

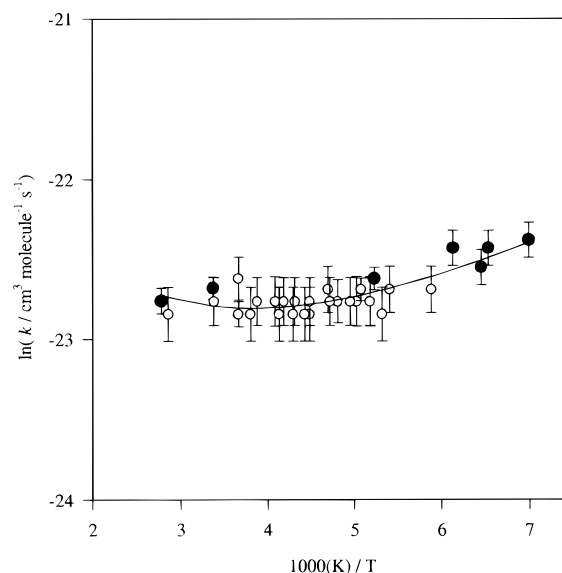


**Figure 4.** Arrhenius plot of the experimental data for  $\text{C}_2\text{H} + \text{C}_2\text{H}_2$ ; (●) this work; (○) data taken from ref 2. The fit to all the data is given by  $8.6 \times 10^{-16} T^{1.8} \exp[(474 \pm 90)/T] \text{ cm}^3 \text{ molecule}^{-1} \text{ s}^{-1}$ .

Table 2 summarizes the kinetic measurements in these experiments for  $k_{\text{CH}_4}$  and  $k_{\text{CD}_4}$  from 154 to 359 K. The data indicate that the rate coefficients  $k_{\text{CH}_4}$  and  $k_{\text{CD}_4}$  have a positive temperature dependence from 154 to 359 K, which can be expressed as  $k_{\text{CH}_4} = (1.2 \pm 0.1) \times 10^{-11} \exp[(-491 \pm 12)/T]$  and  $k_{\text{CD}_4} = (8.7 \pm 1.8) \times 10^{-12} \exp[(-650 \pm 61)/T] \text{ cm}^3 \text{ molecule}^{-1} \text{ s}^{-1}$ , respectively; see Figure 6. The reaction of  $\text{C}_2\text{H} + \text{CD}_4$  exhibits a significant kinetic isotope effect at 300 K of  $k_{\text{CH}_4}/k_{\text{CD}_4} = 2.5 \pm 0.2$ .

## Discussion

Previous measurements of the reaction  $\text{C}_2\text{H} + \text{CH}_4$  were performed at room temperature and are summarized in Table 3. Rendlund *et al.* monitored the  $\text{CH}$  (A-X) product chemiluminescence from the  $\text{C}_2\text{H} + \text{O}_2$  reaction with and without  $\text{CH}_4$ .<sup>11</sup> They measured a room temperature value of  $k_{\text{CH}_4} = (4.8 \pm 1.0) \times 10^{-12} \text{ cm}^3 \text{ molecule}^{-1} \text{ s}^{-1}$ . Okabe photolyzed  $\text{C}_2\text{H}_2$  at 147 nm and determined a ratio of  $k_{\text{CH}_4}/k_{\text{C}_2\text{H}_2} = 0.032 \pm 0.0018$ . Using the present value of  $k_{\text{C}_2\text{H}_2}$  at room temperature of  $(1.3 \pm 0.2) \times 10^{-10} \text{ cm}^3 \text{ molecule}^{-1} \text{ s}^{-1}$ , one obtains a value for  $k_{\text{CH}_4}$  of  $4.2 \times 10^{-12} \text{ cm}^3 \text{ molecule}^{-1} \text{ s}^{-1}$ .<sup>12</sup> Laufer photolyzed

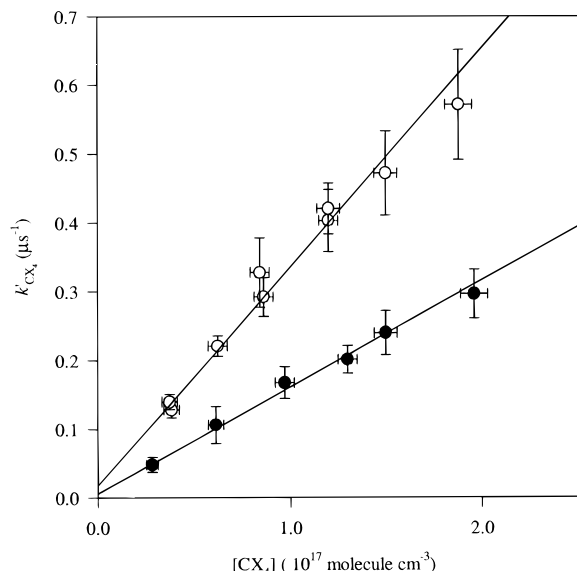


**Figure 5.** Plot of  $k'_{CX_4}$  versus  $[CX_4]$  at 359 K: (○) C<sub>2</sub>H + CH<sub>4</sub>; (●) C<sub>2</sub>H + CD<sub>4</sub>. The rate constants  $k_{CH_4}$  and  $k_{CD_4}$  are equal to  $(3.1 \pm 0.4) \times 10^{-12}$  and  $(1.5 \pm 0.2) \times 10^{-12}$  cm<sup>3</sup> molecule<sup>-1</sup> s<sup>-1</sup>, respectively.

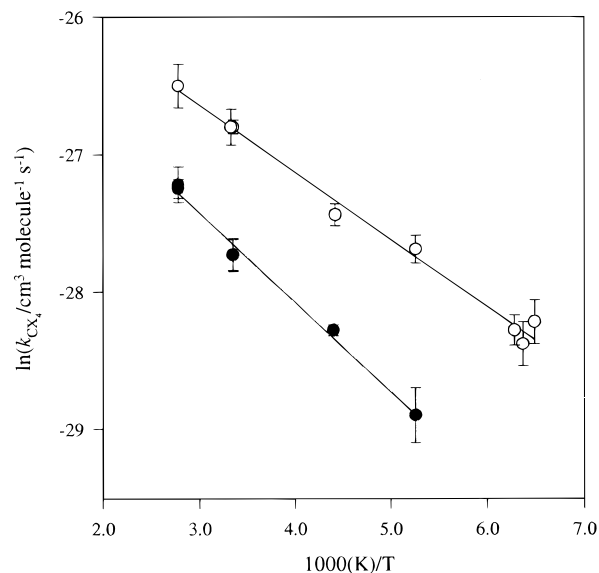


**Figure 6.** Arrhenius plot of C<sub>2</sub>H + CX<sub>4</sub>: (○) C<sub>2</sub>H + CH<sub>4</sub>; (●) C<sub>2</sub>H + CD<sub>4</sub>. The Arrhenius fits for  $k_{CH_4}$  and  $k_{CD_4}$  are given by  $(1.2 \pm 0.1) \times 10^{-11} \exp[(-491 \pm 12)/T]$  and  $(8.7 \pm 1.8) \times 10^{-12} \exp[(-650 \pm 61)/T]$  cm<sup>3</sup> molecule<sup>-1</sup> s<sup>-1</sup>, respectively.

**TABLE 2: Summary of Rate Constants for C<sub>2</sub>H + CH<sub>4</sub> (CD<sub>4</sub>) from 154 to 359 K**

temp (K)	$k_{CH_4}$ (cm <sup>3</sup> molecule <sup>-1</sup> s <sup>-1</sup> )	temp (K)	$k_{CD_4}$ (cm <sup>3</sup> molecule <sup>-1</sup> s <sup>-1</sup> )
359	$(3.1 \pm 0.4) \times 10^{-12}$	359	$(1.5 \pm 0.2) \times 10^{-12}$
300	$(2.3 \pm 0.1) \times 10^{-12}$	300	$(0.9 \pm 0.1) \times 10^{-12}$
226	$(1.2 \pm 0.1) \times 10^{-12}$	227	$(5.2 \pm 0.1) \times 10^{-13}$
190	$(8.7 \pm 0.2) \times 10^{-13}$	190	$(2.8 \pm 0.6) \times 10^{-13}$
159	$(5.2 \pm 0.6) \times 10^{-13}$		
157	$(4.7 \pm 1.0) \times 10^{-13}$		
154	$(5.5 \pm 1.0) \times 10^{-13}$		

CF<sub>3</sub>C<sub>2</sub>H in the presence of CH<sub>4</sub>, and the product [C<sub>2</sub>H<sub>2</sub>] was monitored by absorption at 152 nm over time.<sup>13</sup> Laufer obtained a  $k_{CH_4} = (1.2 \pm 0.2) \times 10^{-12}$  cm<sup>3</sup> molecule<sup>-1</sup> s<sup>-1</sup>. Finally, Lander *et al.* used a diode laser to measure the transient depletion of C<sub>2</sub>H ( $X^2\Sigma^+(0,0,0)$ ) in absorption.<sup>14</sup> They measured a  $k_{CH_4} = (3.0 \pm 0.3) \times 10^{-12}$  cm<sup>3</sup> molecule<sup>-1</sup> s<sup>-1</sup> at 300 K.

The present rate coefficient measurements for C<sub>2</sub>H + CH<sub>4</sub> at 300 K and from 154 to 359 K are  $k_{CH_4} = (2.3 \pm 0.1) \times$

**TABLE 3: Summary of Rate Constants for C<sub>2</sub>H + CH<sub>4</sub> at Room Temperature**

ref	$k_{CH_4}$ (cm <sup>3</sup> molecule <sup>-1</sup> s <sup>-1</sup> )	temp (K)
this work	$(2.3 \pm 0.1) \times 10^{-12}$	300
Renlund <sup>11</sup>	$(4.8 \pm 1.0) \times 10^{-12}$	298
Laufer <sup>13</sup>	$(1.2 \pm 0.2) \times 10^{-12}$	297
Okabe <sup>12</sup>	$4.2 \times 10^{-12a}$	298
Lander <sup>14</sup>	$(3.0 \pm 0.3) \times 10^{-12}$	298

<sup>a</sup> Recalculated using the measured ratio and the present-day C<sub>2</sub>H + C<sub>2</sub>H<sub>2</sub> rate constant  $(1.3 \pm 0.2) \times 10^{-10}$  cm<sup>3</sup> molecule<sup>-1</sup> s<sup>-1</sup>.

$10^{-12}$  and  $k_{CH_4} = (1.2 \pm 0.1) \times 10^{-11} \exp[(-491 \pm 12)/T]$  cm<sup>3</sup> molecule<sup>-1</sup> s<sup>-1</sup>, respectively. From the Arrhenius fit, the energy of activation for C<sub>2</sub>H + CH<sub>4</sub> is equal to  $4.3 \pm 0.1$  kJ mol<sup>-1</sup>. Rate coefficient measurements for C<sub>2</sub>H + CD<sub>4</sub> at 300 K and from 227 to 359 K result in a  $k_{CD_4} = (0.9 \pm 0.1) \times 10^{-12}$  and  $k_{CD_4} = (8.7 \pm 1.8) \times 10^{-12} \exp[(-650 \pm 61)/T]$  cm<sup>3</sup> molecule<sup>-1</sup> s<sup>-1</sup>, respectively. The energy of activation for C<sub>2</sub>H + CD<sub>4</sub> from 227 to 359 K is equal to  $5.4 \pm 0.5$  kJ mol<sup>-1</sup>. No pressure dependence was found for  $k_{CH_4}$  at 300 K over the experimental range  $(0.4\text{--}2.4) \times 10^{18}$  cm<sup>-3</sup> variation in helium buffer gas (15–75 Torr) and for a methane density of  $0.7 \times 10^{17}$  cm<sup>-3</sup>. Over this number density  $k_{CH_4} = (2.4 \pm 0.2) \times 10^{-12}$  cm<sup>3</sup> molecules<sup>-1</sup> s<sup>-1</sup>. Both of these reactions, C<sub>2</sub>H + CH<sub>4</sub> (CD<sub>4</sub>), show a positive temperature dependence, consistent with reactions involving a hydrogen abstraction as the rate-determining step and a positive activation energy.

Our results are most consistent with those of Lander *et al.* Both experiments monitor the direct disappearance of C<sub>2</sub>H. The difference in  $k_{CH_4}$  at 300 K between this work and the work by Lander *et al.* can be attributed to experimental error in determining number density and error in fitting the observed signal. In the experiment by Renlund *et al.* the chemiluminescence of CH ( $A^2\Delta$ ) produced by the reaction C<sub>2</sub>H + O<sub>2</sub> was used to monitor [C<sub>2</sub>H]. They were able to measure  $k_{CH_4}$  by keeping the concentration of O<sub>2</sub> constant while varying the concentration of CH<sub>4</sub>. Renlund *et al.* measured a value for  $k_{CH_4}$  at 300 K that is a factor of 2 greater than the rate constant reported in this work. They reported in a later publication that the reason for the larger  $k_{CH_4}$  was due to vibrationally and/or electronically excited C<sub>2</sub>H producing the CH ( $A^2\Delta$ -X<sup>2</sup>Π) emission.<sup>15</sup> Okabe measured  $k_{CH_4}/k_{C_2H_2}$  to be  $0.032 \pm 0.0018$ . This leads to a value of  $k_{CH_4}$  that is  $\sim 2$  times faster at room temperature than the  $k_{CH_4}$  reported in this work when using  $(1.3 \pm 0.2) \times 10^{-10}$  cm<sup>3</sup> molecule<sup>-1</sup> s<sup>-1</sup> for  $k_{C_2H_2}$ . However, Okabe's result involved measuring  $\phi^0_{C_4H_2}/\phi_{C_4H_2}$ , which is the quantum yield ratio of diacetylene without ( $\phi^0_{C_4H_2}$ ) and with ( $\phi_{C_4H_2}$ ) CH<sub>4</sub> in the mixture and not a direct measurement of the reaction of C<sub>2</sub>H with CH<sub>4</sub>.

The work presented here on C<sub>2</sub>H + C<sub>2</sub>H<sub>2</sub> further supports the reasoning that C<sub>4</sub>H<sub>3</sub><sup>+</sup> is formed via an addition mechanism with no barrier to formation. The short-lived intermediate then immediately dissociates to C<sub>4</sub>H<sub>2</sub> + H. A previous study on C<sub>2</sub>H + C<sub>2</sub>H<sub>2</sub> by this lab reported that within experimental error there was no temperature dependence over 170–350 K.<sup>3</sup> More recent results by Van Look *et al.* also showed no evidence for a temperature dependence from 295 to 450 K.<sup>16</sup> They measured rate coefficients of the reaction C<sub>2</sub>H + O<sub>2</sub> by monitoring CH- ( $A^2\Delta \rightarrow X^2\Pi$ ) chemiluminescence. The rate coefficients for C<sub>2</sub>H with C<sub>2</sub>H<sub>2</sub> were taken from the y-intercepts of their  $k'$  versus [O<sub>2</sub>] plots. An Arrhenius fit to their data is reported as  $k_{C_2H_2} = (1.3 \pm 0.2) \times 10^{-10} \exp[(0 \pm 10)/T]$  cm<sup>3</sup> molecule<sup>-1</sup> s<sup>-1</sup>. Despite previous measurements for the rate coefficients of C<sub>2</sub>H + C<sub>2</sub>H<sub>2</sub>, which show no definite temperature dependence above room temperature,<sup>3,9,16,17</sup> new data presented in this study

does reveal a small negative temperature dependence in the rate coefficients for  $\text{C}_2\text{H} + \text{C}_2\text{H}_2$ .

The measured kinetic isotope effect at 300 K is  $k_{\text{CH}_4}/k_{\text{CD}_4} = 2.5 \pm 0.2$ . Unfortunately, no transition-state calculations have been done on this reaction to be able to compare theory with experiment. Judging by the magnitude of the isotope effect and the reaction mechanism involved, the reaction  $\text{C}_2\text{H} + \text{CH}_4$  ( $\text{CD}_4$ ) exhibits a large primary isotope effect in which the main contribution is the difference in zero-point energies between the initial states and the transition states.<sup>18–20</sup> Hopefully this research will encourage theoretical studies of  $\text{C}_2\text{H} + \text{CH}_4$  ( $\text{CD}_4$ ) for comparison.

In addition to the kinetic isotope effect, there is the possibility for tunneling to occur in this reaction between the H (D) atom of methane and the carbon atom of the  $\text{C}_2\text{H}$  radical. Unfortunately, no curvature is detected in the Arrhenius plot over 154–359 K. This does not eliminate the possibility of tunneling taking place. If the experiment could be done over a larger temperature range, the possibility of detecting curvature in the Arrhenius plot would be more favorable.

Results based on the effect of reaction 2 on photochemical models of Titan are forthcoming. There is little question that this reaction plays a key role in determining the ethane concentration on Titan, but recent experiments by Mordaunt *et al.*<sup>21</sup> have uncovered a new  $\text{CH}_4$  photolysis channel that will affect current photochemical models. Mordaunt *et al.* have shown that the direct photodissociation of  $\text{CH}_4$  to  $\text{CH}_3 + \text{H}$  is the main source of methyl radicals in Titan's atmosphere. Both the discovery by Mordaunt *et al.* and the data in this work should help to clarify the production of ethane in Titan's atmosphere. Updated versions<sup>2</sup> of the Yung *et al.*<sup>1</sup> model and more low-temperature rate coefficients of pertinent reactions are needed to determine whether a complete analysis will match forthcoming spacecraft observations.

**Acknowledgment.** We gratefully acknowledge the National Aeronautics and Space Administration for support of this research and the Department of Energy for additional support.

## References and Notes

- (1) Yung, Y. L.; Allen, M.; Pinto, J. P. *Astrophys. J. Suppl. Ser.* **1984**, 55, 465.
- (2) Toublanc, D.; Parisot, J. P.; Brillet, J.; Gautier, D.; Raulin, F.; McKay, C. P. *Icarus* **1995**, 2, 113.
- (3) Pedersen, J. O. P.; Opansky, B. J.; Leone, S. R. *J. Phys. Chem.* **1993**, 97, 6822.
- (4) Coustenis, A.; Bezard, B.; Gautier, D. *Icarus* **1989**, 80, 54.
- (5) Coustenis, A.; Bezard, B.; *Vis. Astron.* **1991**, 34, 11.
- (6) Opansky, B. J.; Seakins, P. W.; Pedersen, J. O. P.; Leone, S. R. *J. Phys. Chem.* **1993**, 97, 8583.
- (7) Shin, K. S.; Michael, J. V. *J. Phys. Chem.* **1991**, 95, 5864.
- (8) Satyapal, S.; Bersohn, R. *J. Phys. Chem.* **1991**, 95, 8004.
- (9) Farhat, S. K.; Morter, C. L.; Glass, G. P. *J. Phys. Chem.* **1993**, 97, 12789.
- (10) Hall, J. L.; Lee, S. A. *Appl. Phys. Lett.* **1976**, 29, 367.
- (11) Renlund, A. M.; Shokoohi, F.; Reisler, H.; Wittig, C. *Chem. Phys. Lett.* **1981**, 84, 293.
- (12) Okabe, H. *J. Phys. Chem.* **1981**, 75, 2772.
- (13) Laufer, A. H. *J. Phys. Chem.* **1981**, 85, 3828.
- (14) Lander, D. R.; Unfried, K. G.; Glass, G. P.; Curl, R. F. *J. Phys. Chem.* **1990**, 94, 7759.
- (15) Shokoohi, F.; Watson, T. A.; Reisler, H.; Kong, F.; Renlund, A. M.; Wittig, C. *J. Phys. Chem.* **1986**, 90, 5695.
- (16) Van Look, H.; Peeters, J. *J. Phys. Chem.* **1995**, 99, 16284.
- (17) Koshi, M.; Fukuda, K.; Kamiya, K.; Matsui, H. *J. Phys. Chem.* **1992**, 96, 9839.
- (18) Westheimer, F. T. *Chem. Rev.* **1961**, 61, 265.
- (19) *Isotope Effect in Chemical Reactions*; Collins, C. J.; Bowman, N. S., Eds.; Van Nostrand Reinhold: New York, 1970.
- (20) *The Tunnel Effect in Chemistry*; Bell, R. P., Ed.; Chapman Hall: New York, 1980.
- (21) Mordaunt, D. H.; Lambert, I. R.; Morley, G. P.; Ashfold, N. M. R.; Dixon, R. N.; Western, C. M. *J. Chem. Phys.* **1993**, 98, 2054.

JP9532677